Poly (maleic anhydride-alt-1-alkenes) directly grafted to γ-alumina for high-performance organic solvent nanofiltration membranes

Amirilargani, Mohammad; Merlet, Renaud B.; Nijmeijer, Arian; Winnubst, Louis; de Smet, Louis C.P.M.; Sudhölter, Ernst J.R.

Important note
To cite this publication, please use the final published version (if applicable).
Please check the document version above.

Poly (maleic anhydride-*alt*-1-alkenes) directly grafted to γ-alumina for high-performance organic solvent nanofiltration membranes

Mohammad Amirilargani[a,*], Renaud B. Merlet[b], Arian Nijmeijer[b], Louis Winnubst[b], Louis C.P.M. de Smet[a,c], Ernst J.R. Sudhölter[a,*]

[a] *Organic Materials and Interfaces, Department of Chemical Engineering, Delft University of Technology, Van der Maasweg 9, 2629 HZ Delft, the Netherlands*
[b] *Inorganic Membranes, MESA+ Institute for Nanotechnology, University of Twente, P.O. Box 217, 7500 AE Enschede, the Netherlands*
[c] *Laboratory of Organic Chemistry, Wageningen University & Research, Stippeneng 4, 6708 WE Wageningen, the Netherlands*

ABSTRACT

In this study we describe a novel and simple method to couple covalently poly (maleic anhydride-*alt*-1-alkenes) to γ-alumina nanofiltration membranes for the first time. The 1-alkenes varied from 1-hexene, 1-decene, 1-hexadecane to 1-octadecene. The grafting reaction was between the reactive anhydride moieties of the polymer and surface hydroxyl groups, resulting in highly stable bonds. The modified membranes were investigated for their permeation and rejection performance of Sudan Black (SB, M_w 457 Da) in either toluene or ethyl acetate (EA) solution, and very high rejections (> 90%) and high permeation flux were observed compared to un-modified membranes. Initially, the SB in toluene solution was found to bind strongly to the surface hydroxyl groups of the unmodified membranes, an effect not observed in EA solution.

1. Introduction

Nanofiltration is a pressure-driven, membrane-based separation technique with performance properties between those of ultrafiltration (UF) and reverse osmosis (RO) membranes [1,2]. Organic solvent nanofiltration (OSN) is a young separation technique with applications ranging from the recovery of homogeneous catalysts to the purification of organic solvents [3–7]. For such applications a high chemical, mechanical and thermal membrane stability, an excellent long-time performance, and a limited pre-treatment and maintenance are often desired [8].

As polymer-based membranes have a tendency to swell or even dissolve in organic solvents, the use of ceramic membranes for OSN has therefore been growing rapidly in recent years [9–12]. Ceramic membranes show the desired high mechanical strength, are resistant to compaction and do not swell. Despite these superior properties the presence of surface hydroxyl groups makes them hydrophilic which limits their use in non-aqueous media.

A challenging strategy to overcome this limitation is by masking the surface hydroxyl groups by chemical modification with organic monolayers or polymers [3,13,14]. The resulting hybrid organic-ceramic membranes combine the best of two worlds: the superior properties of ceramics with tuned surface properties by proper organic/

polymer chemistry. While the fabrication of hybrid organic-inorganic membranes with incorporated nanoparticles has been widely studied [15–20], hybrid polymeric-ceramic membranes in the area of OSN are much less explored. Such hybrid membranes can be obtained by two different methods. Firstly, by *in-situ* modification of ceramic membranes via sol-gel techniques, where the modification takes place during the selective layer preparation step. Secondly, by post modification of the ceramic membranes with polymers [11,21–26]. The grafting of organic/polymeric moieties to alumina membranes has proven to be a convenient post-modification technique to adjust and control the membrane properties [13]. The surface OH groups are first treated with a primer acting as a linker/coupling agent between the surface OH and the organic/polymer moiety [27,28]. In order to obtain this first step, various silane coupling agents have been investigated [29,30]. For instance, 3-amino propyl triethoxy silane (APTES) and 3-mercapto propyl triethoxy silane (MPTES) were used as linker for the covalent grafting of polydimethylsilane (PDMS) to γ-alumina membranes [13,31–33].

We have now explored the application of maleic anhydride-*alt*-1-alkenes alternating copolymers in the modification of inorganic membranes for the first time. The maleic anhydride unit is highly reactive towards surface OH-groups, enabling direct covalent polymer coupling, thus without the use of a linker unit. In addition, the 1-alkene unit can

---

be varied from short chain to long chain alkenes, enabling tuning of the affinity of the functionalized membranes with various organic solvents. Here, we have investigated a series of four copolymers: three tailor-made alternating copolymers using 1-hexene to 1-hexadecene and one commercially available copolymer containing a hydrophobic block based on 1-octadecene. The (physico-) chemical properties of these compounds are studied in detail, before providing a comprehensive investigation on the performance of γ-alumina membranes grafted with these copolymers.

2. Experimental section

2.1. Materials

All chemicals were purchased from Sigma-Aldrich, unless otherwise indicated. 1-Hexene ($\geq$ 99%), 1-octene (98%), 1-decene (purum, $\geq$ 97%, Fluka) and 1-hexadecene ($>$ 99%, TCI Europe N.V.) were used for the alternating copolymerization reaction. 2,2′-Azo-*bis*-iso-butyronitrile (AIBN) (purum, $\geq$ 98%) was recrystallized twice from methanol. Maleic anhydride (MA) (puriss, $\geq$ 99%) was purified before use by recrystallization from anhydrous benzene and followed by sublimation. Poly(maleic anhydride-*alt*-1-octadecene) (number-average molecular weight M_n: 30–50 kDa). Flat disc-shaped α-alumina membranes (having a diameter of 39 mm, a thickness of 2 mm, and a pore diameter of 80 nm) supporting a thin (3 μm) γ-alumina layer (mean pore diameter of 5 nm), and mesoporous γ-alumina flakes with a pore diameter of ca. 5 nm, were all purchased from Pervatech B.V., The Netherlands.

2.2. Copolymerization procedure

MA (50 mmol), AIBN (0.5 mmol) and the respective 1-alkene (C₆, C₁₀ and C₁₆) (50 mmol) were dissolved in anhydrous 1,4-dioxane (10 ml). The reaction mixture was then deaerated by a freeze-thaw method (3×) and sealed under argon atmosphere. Typically, the reaction proceeded for 4 h at 70 °C after which the reaction solution was added dropwise to methanol (100 ml, 5 °C). The precipitated polymers were collected by filtration, and reprecipitated from a tetrahydrofuran (THF) solution by pouring into methanol (5 °C). The solid material was dried for 24 h at 30 °C under vacuum. The obtained alternating copolymers of MA and 1-alkenes are further referred as P(MA-*alt*-C$_X$) where X indicates the number of carbon atoms of the used alkene.

2.3. Grafting to γ-alumina flakes and supported γ-alumina membranes

The unmodified γ-alumina membranes were washed with water and soaked in ethanol/water (2:1, vol) mixture for 24 h at room temperature to clean the surface. Then, the membranes were dried at 100 °C for 12 h under vacuum and subsequently dipped into a stirred 0.2 wt% solution of the different alternating copolymers in acetone for 12 h. Any contact between the membrane and the magnet stirrer bar was prevented. The samples were washed with pure acetone (3 times). Each membrane sample was subsequently treated at a temperature of 10 °C above their respective glass transition temperature (T_g; see Fig. S6) for 3 h. To remove any non-grafted alternating copolymers, the membranes were washed with acetone for 12 h in a Soxhlet apparatus. The same grafting procedure of the P(MA-*alt*-C$_X$) copolymers was performed for grafting to the unmodified γ-alumina flakes. A schematic diagram of the whole modification procedure is shown in Fig. 1. As shown, nucleophilic attack by the surface hydroxyl groups promotes ring opening of maleic anhydride and esterification reaction, resulting in carboxyl group formation. The membranes grafted with different copolymers are further referred to as γ-alumina-*g*-C$_X$, where X has the meaning as indicated before.

2.4. Characterization

2.4.1. Materials characterization

The number average molecular weight (M_n) of the different synthesized alternating copolymers was determined by gel permeation chromatography (GPC) in a mixture of THF: acetic acid (9:1, vol.) as eluent (flow rate: 1 ml min^{-1}, at 40 °C). The molecular weight and polydispersity index (PDI = M_w/M_n) were calibrated with polystyrene (PS) standards. Proton nuclear magnetic resonance (^{1}H-NMR) spectra of the different alternating copolymers in CDCl₃ were recorded at room temperature using a 400 MHz pulsed Fourier Transform NMR spectrometer (Agilent 400-MR DD2). Fourier transform infrared (FTIR) spectra of the different alternating copolymers in KBr tablets were measured using a Nicolet iS50 FTIR (Thermo Fisher Scientific Co., Madison, USA) spectrophotometer in the range of 4000–500 cm^{-1}. Each spectrum was captured by 128 scans at a resolution of 4 cm^{-1}. The thermogravimetric properties of the modified γ-alumina flakes were determined by a thermogravimetric analyzer (TGA; Mettler Toledo, TGA/SDTA 851e). The samples were heated under a N₂ atmosphere from 25 to 850 °C at a heating rate of 10 °C min^{-1}. The glass transition temperatures (T_g) of the different alternating copolymers were determined under an N₂ atmosphere using a Perkin Elmer 6000 differential scanning calorimeter (DSC). The samples were first heated to 250 °C and then cooled to 25 °C, before the DSC recordings started by heating to 250 °C at a heating rate of 10 °C min^{-1}. N₂ adsorption-desorption experiments were performed at − 196 °C for both the unmodified and copolymers grafted γ-alumina flakes, using a Gemini System VII apparatus. The surface areas were determined by using the Brunauer-Emmet-Teller (BET) method, while the pore size distributions were determined from the desorption branch of the isotherm by the Barret-Joyner-Halenda (BJH) method. The effects of surface modification on the morphology and surface roughness was studied by analyzing the membrane surface topology using an atomic force microscope (AFM, NT-MDT, Ntegra). The roughness average (Sa) in a 500 nm × 500 nm area of the membrane surface was determined from three-dimensional AFM images. Energy dispersive X-ray (EDX) analysis was conducted in the low-vacuum mode at 10 kV using JEOL 6010 LA scanning electron microscopy (SEM). The surface wetting properties (hydrophilicity/hydrophobicity) of the differently modified membranes were determined by their static water contact angle using a Krüss FM40 Easy Drop Standard instrument. According to the standard sessile drop method, a drop of water was put on the top surface of the membrane and the contact angle was measured optically using a camera from the initial contact of the water drop. At least two measurements per membrane and three different samples of each membrane were analysed and the average values are reported.

2.4.2. OSN experimental procedure

Freshly grafted membranes were used for our permeation experiments. These experiments were carried out at a transmembrane pressure (TMP) of 8 bar at room temperature using a dead-end pressure cell made from stainless steel (purchased from Pervatech B.V.). The system is pressurised using inert argon. Prior to each experiment, the membranes were preconditioned with the organic solvent for 12 h. The effective area of each membrane was 8.9 cm² and at least three different samples of each membrane type were tested to study the reproducibility. The model solution to be separated was composed of 20 mg L^{-1} of Sudan Black (SB) in either ethyl acetate (EA) or toluene. During the permeation, the feed solution was stirred at 400 rpm to minimize concentration polarization. The membrane cell was filled with 50 ml of feed solution per membrane and 20 ml (*i.e.*, 40% recovery) of the permeate was collected for each membrane at the permeate side. In between the separation experiments, the membrane cell was thoroughly cleaned and the membranes were rinsed with the solvent used before, dipped in absolute ethanol for 8 h and then cleaned in an ultrasonic bath of absolute ethanol for 5 min. Finally, the cleaned membranes were dried in a vacuum oven at 60 °C for 24 h before the next
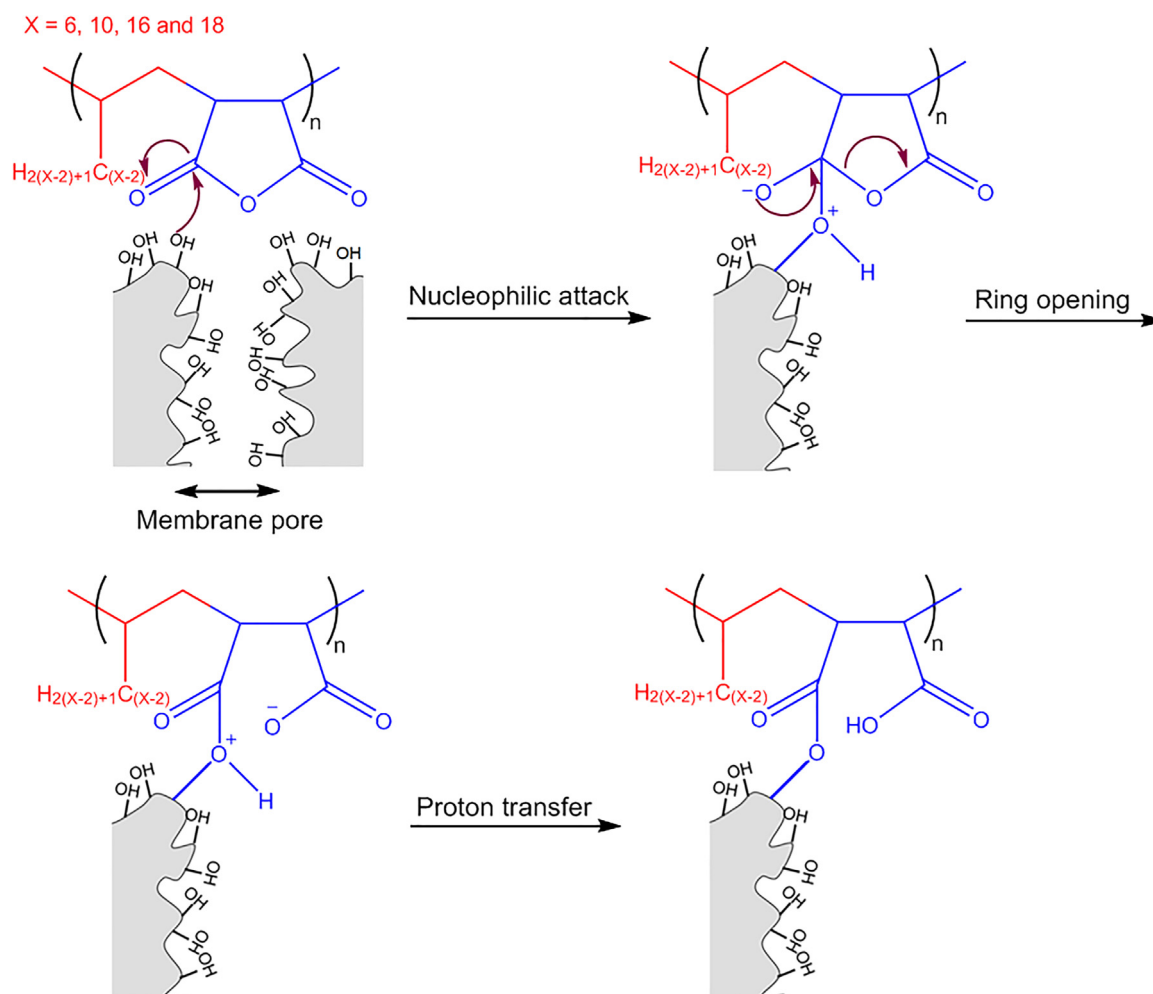
X = 6, 10, 16 and 18

Fig. 1. Schematic diagram showing the grafting process of the alternating copolymers to γ-alumina membranes.

experiment started. The membrane flux was calculated according to Eq. (1) [15],

$$\text{Flux} = J = \frac{V}{At} = [Lm^{-2}h^{-1}] \tag{1}$$

where J is the solvent flux [$L\,m^{-2}\,h^{-1}$], V is the permeate volume [L], A is the effective membrane surface area [m^2] and t is the collecting permeate sample time [h]. The rejections (R) of the SB dye were calculated from the SB concentration in the permeate (C_p) and initial concentration in the feed (C_f), using Eq. (2) [15]:

$$R = \left(1 - \frac{C_p}{C_f}\right) \times 100\% \tag{2}$$

The SB concentrations were determined spectrophotometrically using a double beam UV–Vis spectrophotometer (Shimadzu, UV-1800).

3. Results and discussion

Before discussing the OSN performances of the modified membranes in Section 3.3, we first present and discuss the molecular characterization of the synthesized alternating copolymers and physio-chemical characterization of the copolymer-grafted flakes and membranes in Sections 3.1 and 3.2, respectively.

3.1. Characterization of synthesized alternating copolymers

In Table 1 the number average molecular weight (M_n), weight

Table 1
Molecular weights and PDI values of the MA/α-olefins (C_6–C_{18}) copolymers.

Copolymer	M_w (Da)	M_n (Da)	PDI	N
Poly(MA-*alt*-C$_6$)	27,281	18,272	1.49	100
Poly(MA-*alt*-C$_{10}$)	36,562	23,520	1.55	99
Poly(MA-*alt*-C$_{16}$)	27,644	17,732	1.56	55
Poly(MA-*alt*-C$_{18}$)	28,246	18,230	1.55	81

N = average number of repeating units.

average molecular weight (M_w) and PDI of the alternating copolymers as measured by GPC are shown. The M_w ranges between ~ 27 and ~ 36 Da, and M_n ranges between ~ 17 and ~ 23 kDa. The average number of repeating units is calculated from M_n divided by the molecular weight of the repeating unit. From the used molar ratios of MA and 1-alkene to AIBN initiator in our synthesis procedure, the number of repeating units in the copolymer is expected to be 100. Indeed, for alkene lengths X = 6 and 10 this is observed. For X = 16, the number of repeating units is found to be 55. It is speculated that solubility limitations of the growing polymer chain is accountable for this observation. In addition, the molecular weight was found to be independent of the alkene length used in the polymerization reaction. The same observation was reported before for the alternating copolymers made of MA and different monomers [34–36]. The PDI ranges from 1.49 to 1.56, which is characteristic for free radical polymerizations.

The ^{1}H-NMR spectra of the different copolymers are shown in Figs. S1–S4, ESI†. The obtained results are similar to those reported for
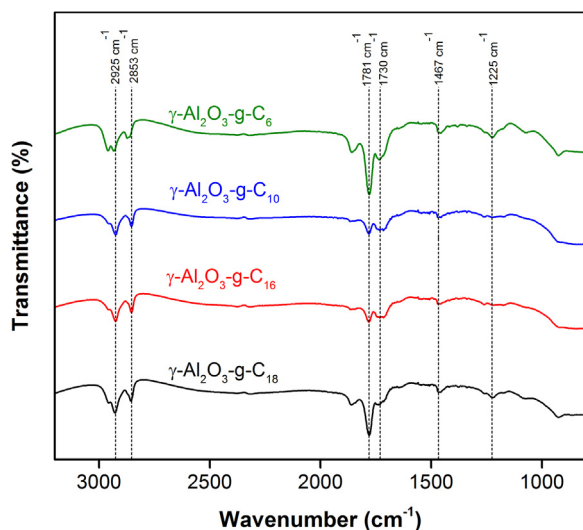
Fig. 2. FTIR spectra of the γ-alumina flakes grafted with different copolymers. The spectra were obtained by subtracting the spectrum of unmodified γ-alumina from each measurement.

copolymers of MA and 1-alkenes [37]. The FTIR spectra of all copolymers used are shown in Fig. S5, ESI†, including a detailed assignment of the most characteristic bands. Finally, the thermal properties of the copolymers synthesized with different 1-alkenes are presented in the Fig. S6, ESI†. The obtained T_g values of the copolymers are in excellent agreement with literature [38].

3.2. Copolymer-grafted flakes and membranes

The FTIR spectra of the copolymer-grafted γ-alumina are shown in Fig. 2. As shown, some characteristic peaks of the copolymers appeared for the grafted flakes. Small peak observed at $1730 \, cm^{-1}$ can be assigned to the C=O bond of esters and carboxylic acids indicating successful grafting. Two peaks observed at 1225 and $1467 \, cm^{-1}$ of can be related to the C-O stretching vibration of the anhydride group of copolymers during the grafting to γ-alumina flakes. They also may attributed to the partially hydrolization of copolymers. The peak observed at $1781 \, cm^{-1}$ is attributed to the stretching vibrations of the carbonyl group and is indicative for anhydride functionality. The peaks at 2925 and $2853 \, cm^{-1}$ can be attributed to the 1-alkene moiety in the copolymers and are clearly presented in the γ-alumina-*g*-copolymers. The observed higher intensity of the peaks for the γ-Al₂O₃-*g*-C₁₈ are attributed to the higher grafting density of C₁₈. Comparing the FTIR spectra between the unmodified and grafted γ-alumina flakes, the latter shows new characteristic peaks belong to alternating copolymers showing the successful grafting of γ-alumina.

The TGA results of the pure γ-alumina flakes and copolymer-grafted flakes are presented in Fig. S7, ESI†. The total weight loss of the unmodified γ-alumina flake was just over 9 wt% at 850 °C, which is attributed to the removal of water molecules trapped inside the nanopores and to the dehydration of surface OH groups. The additional weight loss of the modified γ-alumina flakes is about 1–1.5 wt%, which can be related the loss of copolymers. The weight loss increased by grafting and the loss reached a maximum value of ∼ 10.5 wt% for the γ-alumina-*g*-C₁₈. In addition, γ-alumina-*g*-C₁₀ flakes showed the lowest weight loss of ∼ 10 wt%, indicating the lowest coverage of grafted copolymer of this series.

N₂ adsorption-desorption isotherm showed that the pore size of the grafted flakes are almost the same as those of the unmodified flakes (Fig. S8 and Fig. S9, ESI†). This strongly suggests that only the top surface of the flakes was modified.

TGA results of the unmodified γ-alumina membrane and copolymer-grafted membranes are presented in the Fig. S10, ESI†. The total weight loss of the unmodified membrane was ∼ 0.15% and increased to 0.4–0.5% for the copolymer-grafted membranes. Although, there is no significant difference between the total weight loss of copolymer-grafted membrane, γ-alumina-*g*-C₁₈ membranes showed the highest total weight loss of ∼ 0.5% indicating highest grafting density of poly (MA-*alt*-C₁₈).

AFM analysis was carried out to quantitatively study the roughness and roughness changes at the nanoscale of the unmodified and copolymer-grafted membranes at the nanoscale (Fig. S11, ESI†). In Fig. S11 a ESI†, the image of the unmodified γ-alumina membrane shows a peak-valley structure, while the images of the grafted membranes become smoother as reflected by the reduced S_a values, i.e. the arithmetic average of the 3D roughness. The values of S_a for X = 10 and 16 are less pronounced compared to X = 6 and 18 (Figs. S11 b–e ESI†). Small differences in grafting density may be the reason for that observation, *i.e.* a lower grafting densities lead to a lower reduction of S_a. Indeed for X = 10, it was found that the weight loss in the TGA experiments was lower compared to others, indicating the lower grafting density (Fig. S7 and S10, ESI†).

Low-vacuum mode EDX was performed in this study to analyze the elemental composition of the surface of both unmodified and γ-alumina-*g*-C₁₀ membranes and the results are presented in Fig. 3. The integrity of membrane surface morphology will be preserved in low-vacuum mode EDX as no additional conductive coating is needed. As presented in Figs. 3a and 3b, carbon (C), oxygen (O), aluminium (Al) and phosphorus (P) were found in both unmodified and γ-alumina-*g*-C₁₀. However, the C atom content of the γ-alumina-*g*-C₁₀ is significantly higher than observed for the unmodified membrane. This proves that the membrane surface is covered with copolymer.

The effect of grafting the alternating copolymers to the γ-alumina membranes on the hydrophilic/hydrophobic surface properties was investigated by static water contact angle measurements. Upon grafting, the static water contact angle increases, and this increase is larger for increasing alkyl chain length (X from 6 to 18, see Fig. 4), reflecting an increase of hydrophobicity of the grafted surface. The highest static water contact angle of ∼ 87 degrees was observed for the copolymer carrying the longest alkyl chain unit (X = 18). This water contact angle indicates that the surface is not completely occupied by the alkyl chains. That part of the non-grafted surface OH groups and also the formed carboxylic acid group (COOH) by the anhydride ring opening reaction, contribute to the final surface polarity.

In conclusion, the grafted ceramic membranes show a strongly reduced surface hydrophilicity in comparison to the unmodified membranes.

3.3. OSN performance

The performance of the alternating copolymer-grafted membranes was investigated by permeation of the organic solvents and the rejection of SB solubilised in both EA and toluene. The solvent flux are found to be higher or similar for EA compared to toluene, for both the unmodified and grafted membranes (Fig. 5).

The difference is most pronounced for unmodified membranes. This result indicates a favourable interaction between the hydrophilic alumina pores and the more polar EA compared to the less polar toluene. Grafting reduces the solvent permeation in all cases. The highest flux were observed for C₁₀ and C₁₆, while the solvent flux for C₆ and C₁₈ were somewhat lower. This correlates nicely with our observed differences in the roughness of the grafted surfaces, obtained by AFM and observed total weight loss by the TGA experiments. The C₁₀ and C₁₆-grafted surfaces were less smooth compared to the surfaces grafted by C₆ and C₁₈, explained by a reduced grafting density. This reduced grafting density contributes to the somewhat higher solvent flux.

To quantify the separation performance, UV–vis absorbance spectra of SB in EA and toluene from unmodified and γ-alumina-*g*-C₁₀
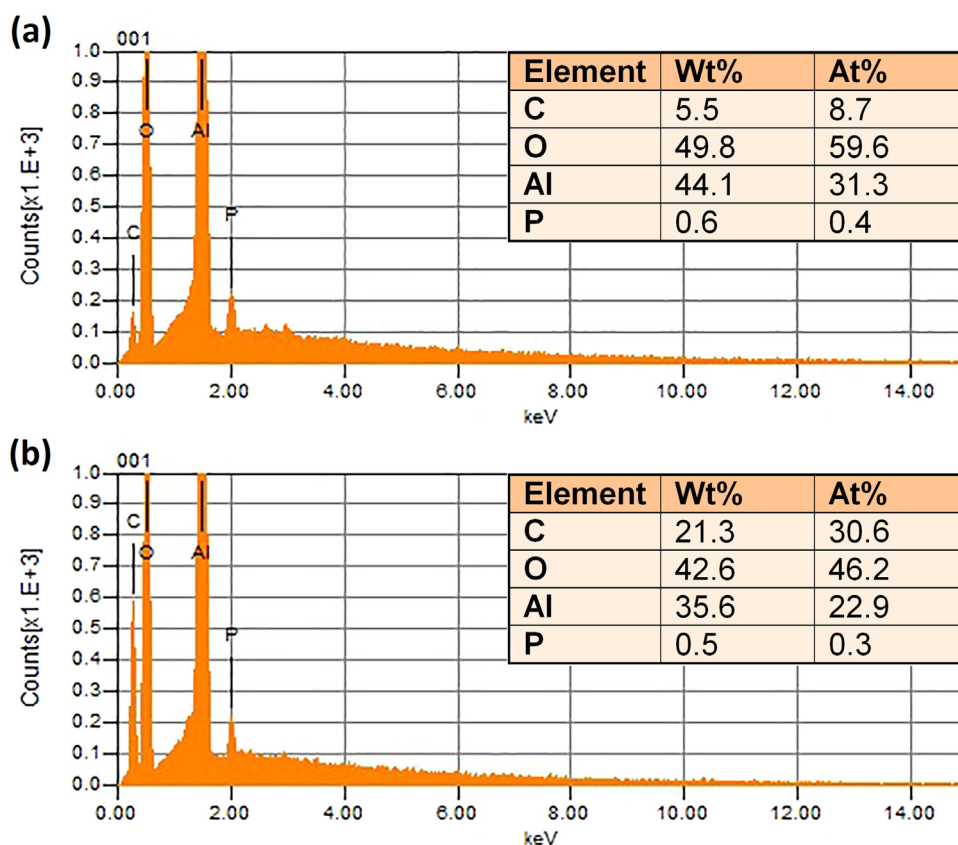
Fig. 3. Elemental analysis of the (a) unmodified and (b) γ-alumina-*g*-C$_{10}$ membrane by EDX.
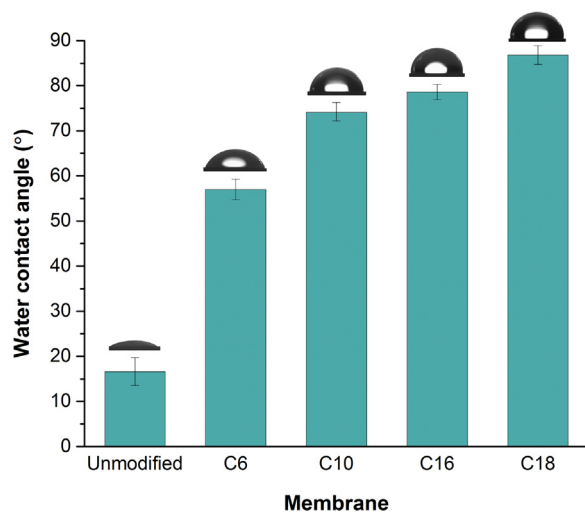
Fig. 4. Water contact angle of unmodified and grafted membranes.

Fig. 5. Solvent flux of the unmodified and alternating copolymer-grafted γ-alumina membranes at TMP of 8 bar.

membranes were obtained as well as optical images of the feed, permeate, and retentate (see Fig. S12, ESI†). The rejection was calculated via Eq. (2) (Section 2.4.2) and the results are presented in Table 2. By using this equation, it is assumed that the amount of SB adsorbed to the membrane is negligible compared to the amounts present in retentate and permeate. The validity of this assumption was checked by making a mass balance of the situation after 40% of recovery. In Table 2 the SB rejection is calculated based on Eq. (2) and the adsorbed amount of SB to the membrane are presented. The adsorbed amount of SB to the membrane was calculated from the mass balance of SB in the initial feed, permeate and retentate, and expressed as percent of the initial SB concentration in the feed phase.
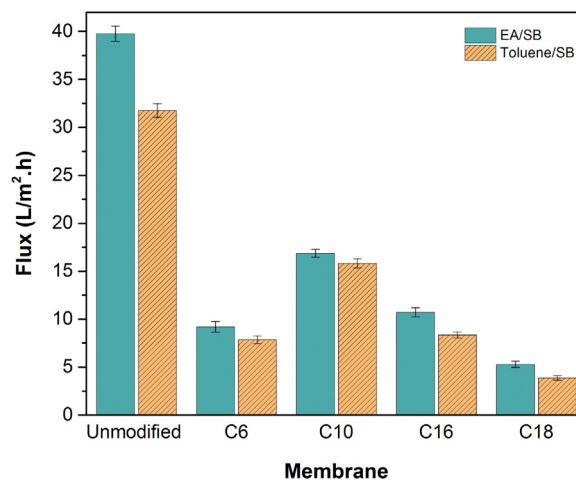
It turns out that for most membranes (unmodified and grafted), 1–6% of the initial SB in the feed solution found to be bound to the membrane. The binding sites are most likely the surface OH groups of the alumina membranes and, for the grafted membranes, the formed carboxylic acid groups (COOH) may also play a role. A remarkably high SB adsorption of 36% is found for the unmodified membrane in toluene solution compared to an adsorption of only 2% in EA solution. This has a serious disturbing effect on the calculated (apparent) rejection of 87%. The reason for this large difference in adsorption might be that the more polar EA binds to the pore surface in competition with SB (thus less SB is bound), while the a polar toluene does not bind strongly to the pore surface, making binding of SB favourable. Also, the earlier

Table 2

Separation performance of unmodified and copolymer-grafted membranes (40% recovery of the feed)[*].

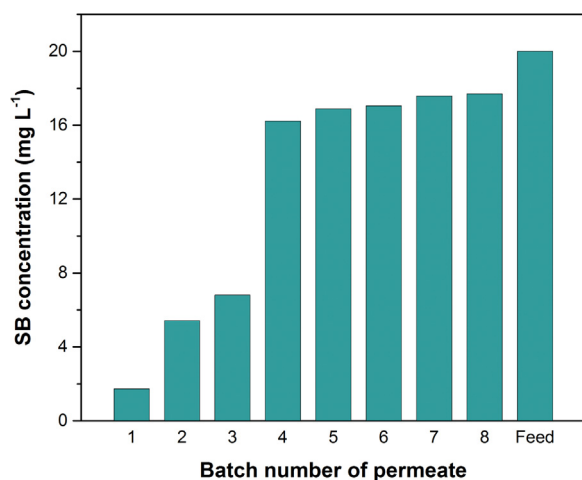| Membrane	SB/EA		SB/Toluene	
	Rejection (%)[†]	Membrane adsorption (%)	Rejection (%)[†]	Membrane adsorption (%)
Unmodified	18 ± 2	2	87 ± 1	36
γ-alumina-*g*-C_6	94 ± 1	5	99 ± 1	3
γ-alumina-*g*-C_{10}	90 ± 1	3	98 ± 1	6
γ-alumina-*g*-C_{16}	91 ± 1	2	99 ± 1	4
γ-alumina-*g*-C_{18}	92 ± 1	4	99 ± 1	1

[*] The model feed solution was a 50 ml mixture of SB (20 mg L^{-1}) in EA and toluene.

[†] The rejection value are calculated based on the Eq. (2), expressing the effects of retention and adsorption of solute by membranes.

mentioned lower grafting coverage by copolymers with X = 10 and 16 (from solvent permeation flux and AFM measurements), is reflected by the higher adsorption of SB in toluene compared to EA. The amount of bound SB of 1–6% is assumed to be an equilibrium value. For these situations the rejections can be calculated reliably, based on permeate concentrations and initial feed concentrations (Table 2). The SB rejection of the copolymer-grafted membranes significantly improved compared to the unmodified membranes. In addition, it was shown that the copolymer-grafted membranes showed slightly higher SB rejection in the presence of toluene compared to EA. The favourable interaction between the polymer grafted surface and toluene compared to EA might be the reason for the higher SB rejection in the presence of toluene than in the presence of EA. Changing the alkene chain length does not show any significant effect on the SB rejection. Our obtained results show that the membrane surface layer properties and the specific solvent/solute interaction with the membrane surface affect the overall performance of OSN membranes [3,39,40].

In order to investigate the adsorption equilibrium, the separation performance of unmodified and γ-alumina-*g*-C_{10} membranes with a higher feed volume (200 ml containing 20 mg L^{-1} SB in toluene) at a TMP of 8 bar was studied. The higher feed volume allows one to investigate whether the adsorption equilibrium is obtained. Different 20 ml batches of permeate were collected separately and analysed by UV–Vis to determine the SB concentration (see Fig. S13, ESI†). The variation of SB concentration for each collected sample of permeate is shown in Fig. 6.

Initially the SB concentration was low (~ 6.8 mg L^{-1} for the batch

number 3), while after 60 ml of permeation (30% recovery), the SB concentration significantly increased to ~ 16.2 mg L^{-1} in the 4th batch. Clearly, after permeating 60 ml, the SB binding sites in the membrane get saturated, and no significant additional loss of SB by binding to the membrane occurred. However the SB concentration in the retentate also might have resulted in a (slight) increase of SB bound to the membrane, as long as the binding sites were not all occupied.

To study the rejection of unmodified and γ-alumina-*g*-C_{10} membranes at different cumulative recoveries, collected batches (20 ml) of permeate were mixed and analysed with UV–Vis (Fig. S14, ESI†). For instance, 20% recovery permeate sample were prepared by mixing of 1st and 2nd batch while for the 30% recovery the 3rd batch was also added.

The UV–Vis absorption spectra of the different cumulative recoveries (from 10 up to 80%) for unmodified membrane reveal that the SB concentration increases with recovery (Fig. S14 a, ESI†). This was not observed for the γ-alumina-*g*-C_{10} membrane as the SB concentration was found to be almost constant at the full range of recoveries (Fig. S14, ESI†). The strong affinity of SB in toluene to the unmodified membrane at the first recoveries results in an initially low SB concentration in the permeate. This affinity is clearly visible by the naked eye (insets in the Fig. S14, ESI†). As during permeation saturation of the adsorption sites on the γ-alumina is approximated, the SB concentration in the permeate increases, and rejection (as a logical consequence) decreases from ~ 87 to ~ 30% (Fig. 7).

The photographs taken from the feed, retentate and permeate with different recoveries are presented in Fig. S15, ESI†.

To gain more insight into the overall OSN performance of the γ-alumina-*g*-copolymer membranes, the performance of a γ-alumina-*g*-C_{10} membrane for purification of EA and toluene was compared with previously reported functionalized ceramic membranes [21,29,41] and commercially polymeric STARMEM 122 membrane [42,43]. These results are summarized in Fig. 8. It is observed that the γ-alumina-*g*-C_{10} has the highest rejection values with comparable EA and toluene flux compared with commercially and previously reported ceramic membranes. Only commercial polydimethylsiloxane (PDMS) with different chain lengths was used in previous work on functionalization of γ-alumina membranes [29]. Generally, PDMS grafted γ-alumina membranes showed higher flux of EA and toluene while their rejection values are significantly lower than observed for the γ-alumina-*g*-C_{10} membrane. It is assumed that PDMS with a short chain length (*Mw*: ~ 1000–1900 Da) is grafted into the internal surface of the pores and narrows the pore diameter. In contrast, in our study the copolymers with higher molecular weight did not graft into the pores. However, the copolymers grafted on the surface of γ-alumina membranes, covered

Fig. 6. SB concentrations from sample to sample for consecutive 20 ml batches of permeate for the unmodified membrane tested with 200 ml of SB/toluene.
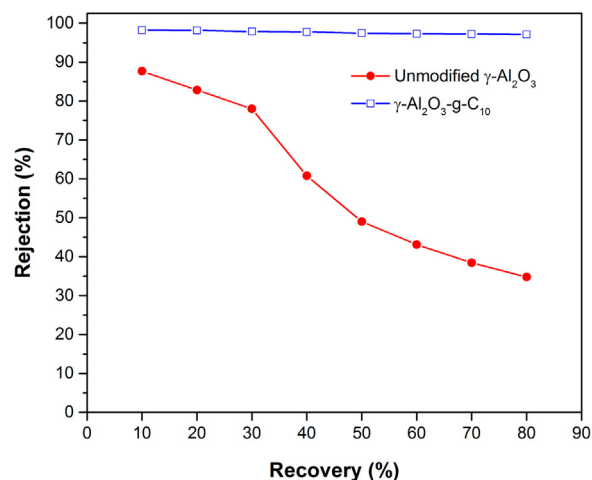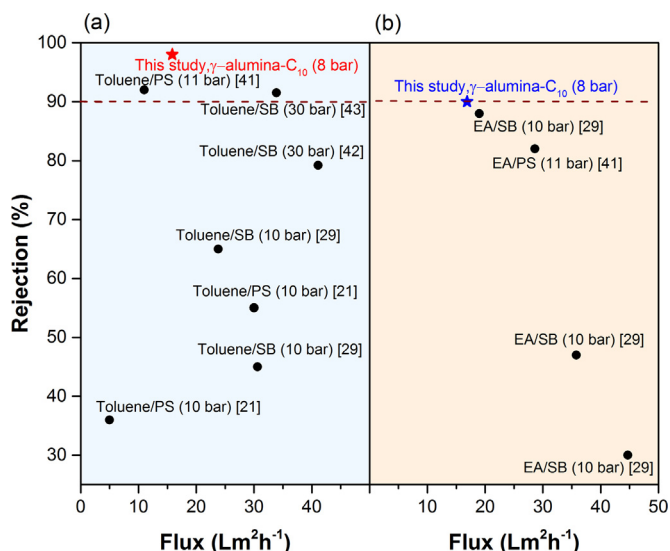

Fig. 7. SB rejection from toluene solution as function of recovery observed for unmodified and γ-alumina-*g*-C_{10} membranes.

Fig. 8. Comparison of the OSN performance of γ-alumina-*g*-C₁₀ membrane with previously reported functionalized ceramic membranes [21,29,41] and commercially polymeric STARMEM 122 membrane [42,43]: (a) SB or polystyrene (PS, M_w 580 Da)/toluene and (b) SB/EA were used as model feed. The dotted line represented 90% solute rejection.

the pores and resulted in lower flux and significantly higher rejection compared with small-chain PDMS grafted γ-alumina.

4. Conclusions

Hybrid organic solvent nanofiltration (OSN) membranes were successfully made by covalent modification of ceramic γ-alumina membranes with alternating copolymers from maleic anhydride and 1-alkenes (hexene, decene, hexadecane, and octadecene). The maleic anhydride unit in the polymer reacts with the surface OH groups of the ceramic membrane and reduces the surface polarity by masking the surface OH groups. The permeation is sensitive to the grafting density as shown by the higher permeation observed for X = 10 and 16 compared to the other, as a result of a somewhat lower grafting density. The modification has a large effect on the increased rejection of Sudan Black (SB) from EA and toluene solution, up to values of 90% and 99%, respectively. For SB in toluene solution it was found that the SB molecules bind more strongly to the surface OH groups present in the unmodified ceramic membrane compared to SB in EA solution. The weaker binding of SB for the EA situation is attributed to a favourable competitive binding of EA with respect to SB for binding to surface OH groups. For SB in toluene the SB binding is more favourable than the toluene binding. By increasing the permeation volume, a situation is obtained where the bound SB to surface OH groups is close to saturation, and for that situation a SB rejection of ∼ 35% was achieved. Covalent modification of the polar γ-alumina membranes by grafting with alternating copolymers of maleic anhydride and 1-alkenes, increases their hydrophobicity and selectivity, rendering such membranes suitable for OSN.

Acknowledgment

from TU Delft for DSC analysis, SEM-EDX, technical and LABVIEW support.

Appendix A. Supplementary material

H-NMR and FTIR spectra and DSC thermograms of different alternating copolymers (Fig. S1–S6), TGA curves, N₂ adsorption-desorption isotherm and Pore size distribution of γ-alumina flakes (Fig. S7–S9), Three-dimensional AFM images (Fig. S11), UV–vis absorption spectra (Fig. S12–S14), Photographs of the feed, retentate and permeate (Fig. S15), BET surface area and mean pore diameter of γ-alumina flakes (Table S1)

Appendix A. Supporting information

Supplementary data associated with this article can be found in the online version at doi:10.1016/j.memsci.2018.07.042.

References

[1] J. Zhang, Y. Hai, Y. Zuo, Q. Jiang, C. Shi, W. Li, Novel diamine-modified composite nanofiltration membranes with chlorine resistance using monomers of 1,2,4,5-benzene tetracarbonyl chloride and m-phenylenediamine, J. Mater. Chem. A 3 (2015) 8816–8824.

[2] J. Zhu, M. Tian, J. Hou, J. Wang, J. Lin, Y. Zhang, J. Liu, B. Van, der Bruggen, surface zwitterionic functionalized graphene oxide for a novel loose nanofiltration membrane, J. Mater. Chem. A 4 (2016) 1980–1990.

[3] M. Amirilargani, M. Sadrzadeh, E.J.R. Sudhölter, L.C.P.M. de Smet, Surface modification methods of organic solvent nanofiltration membranes, Chem. Eng. J. 289 (2016) 562–582.

[4] G. Szekely, M.F. Jimenez-Solomon, P. Marchetti, J.F. Kim, A.G. Livingston, Sustainability assessment of organic solvent nanofiltration: from fabrication to application, Green Chem. 16 (2014) 4440–4473.

[5] A.V. Volkov, G.A. Korneeva, G.F. Tereshchenko, Organic solvent nanofiltration: prospects and application, Russ. Chem. Rev. 77 (2008) 983–993.

[6] F.C. Ferreira, H. Macedo, U. Cocchini, A.G. Livingston, Development of a liquid-phase process for recycling resolving agents within diastereomeric resolutions, Org. Process Res. Dev. 10 (2006) 784–793.

[7] M.G. Buonomenna, J. Bae, Organic solvent nanofiltration in pharmaceutical industry, Sep. Purif. Rev. 44 (2014) 157–182.

[8] S. Rezaei Hosseinabadi, K. Wyns, V. Meynen, R. Carleer, P. Adriaensens, A. Buekenhoudt, B. Van der Bruggen, Organic solvent nanofiltration with Grignard functionalised ceramic nanofiltration membranes, J. Membr. Sci. 454 (2014) 496–504.

[9] X.Q. Cheng, Y.L. Zhang, Z.X. Wang, Z.H. Guo, Y.P. Bai, L. Shao, Recent advances in polymeric solvent-resistant nanofiltration membranes, Adv. Polym. Technol. 33 (2014) 21455.

[10] L.G. Peeva, S. Malladi, A. Livingston, Nanofiltration operations in nonaqueous systems, in: L.G. Drioli (Ed.), Comprehensive Membrane Science and Engineering, Elsevier, Oxford, 2010.

[11] A. Dobrak, B. Verrecht, H. Van den Dungen, A. Buekenhoudt, I.F.J. Vankelecom, B. Van, der Bruggen, Solvent flux behavior and rejection characteristics of hydrophilic and hydrophobic mesoporous and microporous TiO2 and ZrO2 membranes, J. Membr. Sci. 346 (2010) 344–352.

[12] N.F.D. Aba, J.Y. Chong, B. Wang, C. Mattevi, K. Li, Graphene oxide membranes on ceramic hollow fibers – microstructural stability and nanofiltration performance, J. Membr. Sci. 484 (2015) 87–94.

[13] C.R. Tanardi, I.F.J. Vankelecom, A.F.M. Pinheiro, K.K.R. Tetala, A. Nijmeijer, L. Winnubst, Solvent permeation behavior of PDMS grafted γ-alumina membranes, J. Membr. Sci. 495 (2015) 216–225.

[14] C.R. Tanardi, R. Catana, M. Barboiu, A. Ayral, I.F.J. Vankelecom, A. Nijmeijer, L. Winnubst, Polyethyleneglycol grafting of γ-alumina membranes for solvent resistant nanofiltration, Microporous Mesoporous Mater. 229 (2016) 106–116.

[15] J. Campbell, R.P. Davies, D.C. Braddock, A.G. Livingston, Improving the permeance of hybrid polymer/metal-organic framework (MOF) membranes for organic solvent nanofiltration (OSN) - development of MOF thin films via interfacial synthesis, J. Mater. Chem. A 3 (2015) 9668–9674.

[16] J. Campbell, G. Szekely, R.P. Davies, D.C. Braddock, A.G. Livingston, Fabrication of hybrid polymer/metal organic framework membranes: mixed matrix membranes versus in situ growth, J. Mater. Chem. A 2 (2014) 9260–9271.

[17] S. Sorribas, P. Gorgojo, C. Téllez, J. Coronas, A.G. Livingston, High flux thin film nanocomposite membranes based on metal-organic frameworks for organic solvent nanofiltration, J. Am. Chem. Soc. 135 (2013) 15201–15208.

[18] H. Siddique, E. Rundquist, Y. Bhole, L.G. Peeva, A.G. Livingston, Mixed matrix membranes for organic solvent nanofiltration, J. Membr. Sci. 452 (2014) 354–366.

[19] Y. Li, T. Verbiest, I. Vankelecom, Improving the flux of PDMS membranes via localized heating through incorporation of gold nanoparticles, J. Membr. Sci. 428 (2013) 63–69.

[20] K. Vanherck, A. Aerts, J. Martens, I. Vankelecom, Hollow filler based mixed matrix membranes, Chem. Commun. 46 (2010) 2492–2494.

[21] S.R. Hosseinabadi, K. Wyns, A. Buekenhoudt, B. Van der Bruggen, D. Ormerod, Performance of Grignard functionalized ceramic nanofiltration membranes, Sep. Purif. Technol. 147 (2015) 320–328.

[22] T. Tsuru, T. Sudou, S.-i. Kawahara, T. Yoshioka, M. Asaeda, Permeation of Liquids through Inorganic Nanofiltration Membranes, J. Colloid Interface Sci. 228 (2000) 292–296.

[23] T. Tsuru, M. Narita, R. Shinagawa, T. Yoshioka, Nanoporous titania membranes for permeation and filtration of organic solutions, Desalination 233 (2008) 1–9.

[24] T. Tsuru, M. Miyawaki, T. Yoshioka, M. Asaeda, Reverse osmosis of nonaqueous solutions through porous silica-zirconia membranes, AIChE J. 52 (2006) 522–531.

[25] S.M. Dutczak, M.W.J. Luiten-Olieman, H.J. Zwijnenberg, L.A.M. Bolhuis-Versteeg, L. Winnubst, M.A. Hempenius, N.E. Benes, M. Wessling, D. Stamatialis, Composite capillary membrane for solvent resistant nanofiltration, J. Membr. Sci. 372 (2011) 182–190.

[26] X. Li, C.-A. Fustin, N. Lefevre, J.-F. Gohy, S.D. Feyter, J.D. Baerdemaeker, W. Egger, I.F.J. Vankelecom, Ordered nanoporous membranes based on diblock copolymers with high chemical stability and tunable separation properties, J. Mater. Chem. 20 (2010) 4333–4339.

[27] A.F.M. Pinheiro, A. Nijmeijer, V.G.P. Sripathi, L. Winnubst, Chemical modification/grafting of mesoporous alumina with polydimethylsiloxane (PDMS), Eur. J. Chem. 6 (2015) 287–295.

[28] A. Amelio, M. Sangermano, R. Kasher, R. Bernstein, A. Tiraferri, Fabrication of nanofiltration membranes via stepwise assembly of oligoamide on alumina supports: effect of number of reaction cycles on membrane properties, J. Membr. Sci. 543 (2017) 269–276.

[29] C.R. Tanardi, A. Nijmeijer, L. Winnubst, Coupled-PDMS grafted mesoporous γ-alumina membranes for solvent nanofiltration, Sep. Purif. Technol. 169 (2016) 223–229.

[30] X. Qiu, X.-Y. Xu, Y. Liang, H. Guo, The molecularly imprinted polymer supported by anodic alumina oxide nanotubes membrane for efficient recognition of chlor-opropanols in vegetable oils, Food Chem. 258 (2018) 295–300.

[31] A.F.M. Pinheiro, D. Hoogendoorn, A. Nijmeijer, L. Winnubst, Development of a PDMS-grafted alumina membrane and its evaluation as solvent resistant nanofiltration membrane, J. Membr. Sci. 463 (2014) 24–32.

[32] C.R. Tanardi, A.F.M. Pinheiro, A. Nijmeijer, L. Winnubst, PDMS grafting of mesoporous γ-alumina membranes for nanofiltration of organic solvents, J. Membr. Sci. 469 (2014) 471–477.

[33] R.B. Merlet, C.R. Tanardi, I.F.J. Vankelecom, A. Nijmeijer, L. Winnubst, Interpreting rejection in SRNF across grafted ceramic membranes through the Spiegler-Kedem model, J. Membr. Sci. 525 (2017) 359–367.

[34] F. Martínez, E. Uribe, A.F. Olea, Copolymerization of maleic anhydride with styrene and α-Olefins. Molecular and thermal characterization, J. Macromol. Sci. Part A 42 (2005) 1063–1072.

[35] M.H. Nasirtabrizi, Z.M. Ziaei, A.P. Jadid, L.Z. Fatin, Synthesis and chemical modification of maleic anhydride copolymers with phthalimide groups, Int. J. Ind. Chem. 4 (2013) 11.

[36] O. Kudina, O. Budishevska, A. Voronov, A. Kohut, O. Khomenko, S. Voronov, Synthesis of new amphiphilic comb-like copolymers based on maleic anhydride and α-olefins, Macromol. Symp. 298 (2010) 79–84.

[37] M.C. Davies, Controlled Alternating Copolymerisation of Maleic Anhydride and Electron Donating Monomers (Ph.D. Thesis), Loughborough University, 2002.

[38] I.D. Gunbas, Water-borne, Functional Coatings from maleic Anhydridecontaining Copolymers: Chemistry and Phase Behavior (Ph.D. Thesis), Eindhoven University of Technology, 2012.

[39] P. Marchetti, M.F. Jimenez Solomon, G. Szekely, A.G. Livingston, Molecular separation with organic solvent nanofiltration: a critical review, Chem. Rev. 114 (2014) 10735–10806.

[40] X. Li, W. Goyens, P. Ahmadiannamini, W. Vanderlinden, S. De Feyter, I. Vankelecom, Morphology and performance of solvent-resistant nanofiltration membranes based on multilayered polyelectrolytes: study of preparation conditions, J. Membr. Sci. 358 (2010) 150–157.

[41] S.R. Hosseinabadi, K. Wyns, V. Meynen, A. Buekenhoudt, B. Van der Bruggen, Solvent-membrane-solute interactions in organic solvent nanofiltration (OSN) for Grignard functionalised ceramic membranes: explanation via Spiegler-Kedem theory, J. Membr. Sci. 513 (2016) 177–185.

[42] S. Darvishmanesh, J. Degrève, B. Van Der Bruggen, Mechanisms of solute rejection in solvent resistant nanofiltration: the effect of solvent on solute rejection, Phys. Chem. Chem. Phys. 12 (2010) 13333–13342.

[43] S. Darvishmanesh, J. Degrè, B.V.D. Bruggen, Performance of solvent-pretreated polyimide nanofiltration membranes for separation of dissolved dyes from toluene, Ind. Eng. Chem. Res. 49 (2010) 9330–9338.